Hindawi
Advances in Civil Engineering
Volume 2022, Article ID 4255280, 13 pages
https://doi.org/10.1155/2022/4255280

Research Article

Movements and Its In-Process Control of Ground and Built Structures due to Tunnelling in Urban Areas

Dingli Zhang,[1] Liqiang Cao ,[1,2,3] Jianbo Fei,[2,3] Huangcheng Fang,[1] Lin Yu,[1] and Xuefei Hong[1]

[1]*Key Laboratory of Urban Underground Engineering of Ministry of Education, Beijing Jiaotong University, Beijing 100044, China*
[2]*College of Civil and Transportation Engineering, Shenzhen University, Shenzhen 518060, China*
[3]*Underground Polis Academy, Shenzhen University, Shenzhen 518060, China*

Correspondence should be addressed to Liqiang Cao; liqiangcao@szu.edu.cn

Received 28 September 2021; Accepted 3 December 2021; Published 29 January 2022

Academic Editor: Yanbin Luo

Tunnelling-induced environmental responses including ground movements and deformation of the environmental structures are the two prominent issues needed to be carefully disposed in urban areas. This paper tries to develop a theoretical framework to evaluate and control the environmental deformation to avoid two disasters including ground collapse and structural failure. According to the mechanical responses of the ground due to tunnelling, the urban ground in China can be roughly divided into three types including composite multilayered ground, highly water-bearing ground, and mixed rock ground. The displacements of ground and environmental structures due to tunnelling in multilayered ground are emphatically discussed in view of its largest proportion distribution. The cumulative and mutational characteristics of the displacements are considered, which can be the main basis for distinguishing the occurrence of two types of disasters. Based on the development of the displacements, the three-stage evolution model of disaster is established. Combined with the existing displacement and degeneration of the ground and structures and the safety factor, the displacement control standards can be eventually determined. The theoretical framework of in-process control is established which is based on the prediction, measurement, and control standards of the displacements. In the framework, the prediction model can be modified in time, and the tunnelling parameters can be adjusted synchronously. The current research is successfully applied in the Qinghuayuan Tunnel Project.

1. Introduction

With the rapid growth of the urban population, the problem of land shortage and traffic congestion has become increasingly prominent [1, 2]. Underground transportation has become the best option to alleviate this problem [3–5]. The successful construction of underground transportation depends mainly on the successful construction of tunnels [6, 7]. Different from ground surface structures, the applied load of tunnels is hard to be accurately estimated due to the complexity of the mechanical properties of soils [8], thus making the mechanical responses of tunnels ambiguous. Currently, subways are being constructed in all regions of China, from the north [9] to the south [10] and from the west [11] to the east [12]. The soil conditions vary from place to place, thus resulting in different mechanical responses. In addition to the ground conditions, the influence of the tunnel construction method on the mechanical response of the ground is also prominent [13, 14].

The construction method of urban tunnels has been developed from the cut-and-cover method (including bottom-up and top-down sequences) to the mining method. The mining method usually includes the shallow tunnelling method (STM) [15, 16] and the shield method (SM) [17, 18]. Compared with the SM, the STM is more flexible, so it can adapt to any geological conditions and excavation section shape. However, the SM has a higher degree of mechanization and automation, is less affected by human factors, and has a higher construction speed. Besides, due to the development of TBM (tunnel boring machine) technology, the

application range of SM is gradually expanding [19, 20]. The common point of these two methods is that they both inevitably cause ground movements [21, 22] and even ground collapses [23, 24], despite the control measures being well adopted. The propagation of ground movements can also induce deformation, even failure of the existing environmental structures [25, 26]. Therefore, how to evaluate and control the effect of tunnelling on the built environment to avoid ground collapse and structural failure is a crucial topic.

Some scholars have conducted extensive research on the tunnelling-induced displacements of the ground [27–29] and environmental structures [30–32]. Others have performed in-depth analysis on the environmental disasters including ground collapse [33–37] and structural failure [38–40]. Naturally, if the ground deformation is not controlled, it is very easy to induce ground collapse, and if the structural deformation is not controlled, it is prone to cause structural failure. However, few studies have unified the development of deformation with the evolution of the disasters, so the deformation control standards cannot be effectively formulated, which is not conducive to disaster circumvention. In addition, since the development of environmental deformations and the evolution of disasters advance with the progress of tunnelling, in-process control is very important. Relevant scholars have explored this topic using information interaction [41–43]. It brings all parties involved in the project together to facilitate information sharing and communication, and to a certain extent, the probability of disasters is alleviated. However, this way is based on management thinking and lacks the research of control theory which is based on the evolution process of disasters. Therefore, the control of disasters still has great uncertainty.

Regarding the issue above, this paper aims to develop a theoretical framework for disaster control in urban tunnel construction and apply it in actual engineering. We divide the soil in China's urban areas into three typical categories including composite multilayered ground, highly water-bearing ground, and mixed rock ground. The main disaster characteristic of each typical soil is analyzed, with emphasis on the study of composite multilayered ground. Firstly, based on the elastic equivalent theory [44] combined with L & P formula [45], ground movements can be obtained by the semianalytical method [46] when tunnelling in multilayered ground. The volume loss can be calculated based on the double-circle model by considering the tunnelling parameters at the tunnel periphery [21, 47]. Secondly, the mechanical responses of environmental structures due to tunnelling are analyzed using the two-stage method (TSM). Based on the development of the displacements, the evolution of two environmental disasters including ground collapse and structural failure is analyzed. Then, the displacement control standards of ground and environmental structures are determined so as to guarantee safety during the tunnelling process. Finally, the theoretical framework of the in-process feedback control is introduced and applied in the Qinghuayuan Tunnel Project. The current study can offer insights into the prediction and in-process control of movements of ground and built environment when tunnelling in urban areas.

2. Prediction of Ground Movements due to Urban Tunnel Construction

China has a vast territory, and the geological environment of different regions has created different types of ground. Each ground has its own characteristics; therefore, the characteristics of displacement and disaster due to tunnelling of each ground are also different. Nevertheless, according to the mechanical responses of the ground due to tunnelling, the urban ground can be roughly divided into three types including composite multilayered ground, highly water-bearing ground, and mixed rock ground.

2.1. Displacement Characteristics of Three Typical Types of Urban Ground in China. Composite multilayered ground [21] is represented by Beijing, Shenyang, and Chengdu (Figure 1). The formation of the ground is mainly determined by river alluvium and alluvial deposits. For example, the formation of Beijing ground is mainly affected by the alluvium of the Yongding River. The river starts in the northwest mountainous area, and the larger pebbles cannot be carried and deposited in place. Then, the river flows to the southeast, the flow rate gradually slows down, and the smaller fine sand is gradually deposited. With the gradual reduction of the river range, the ground composition is basically fixed. Therefore, the west and north of Beijing are dominated by pebbles and thick sandy soils, and the south and east are dominated by silt, clay, and alternate layers of sand, clay, and pebbles. The characteristic of this kind of ground is the unevenness of the soil layer, such as hard interlayer ground and soft interlayer ground. Soft and hard interlayers have a great influence on ground displacement. The main disasters are ground collapse and the failure of the environmental structures caused by the excessive ground movements.

Highly water-bearing ground [12] is represented by Shanghai, Ningbo, and Tianjin (Figure 1). The formation of the ground is mainly affected by the sedimentation of fine clay soil carried by slow-moving sea water and river water. These cities are basically located in the delta of the sea. For example, the formation of Shanghai ground is mainly due to the sedimentation of the Yangtze River into the sea. The silty clay and abundant groundwater make this type of ground have high compressibility, high rheology, and high consolidation. The characteristic of this kind of ground is abundant of groundwater; therefore, the seepage and consolidation have a great influence on ground movements. The main disasters are water inrush during the excavation process and long-term displacements due to consolidation.

Mixed rock ground [48] is represented by Qingdao, Dalian, and Chongqing (Figure 1). The formation of the ground is mainly affected by geological movement and rock weathering. These cities are always located on the mountain. For example, Qingdao is on the ground which is filled with soil, medium-coarse sand, and the base rock, and the tunnel

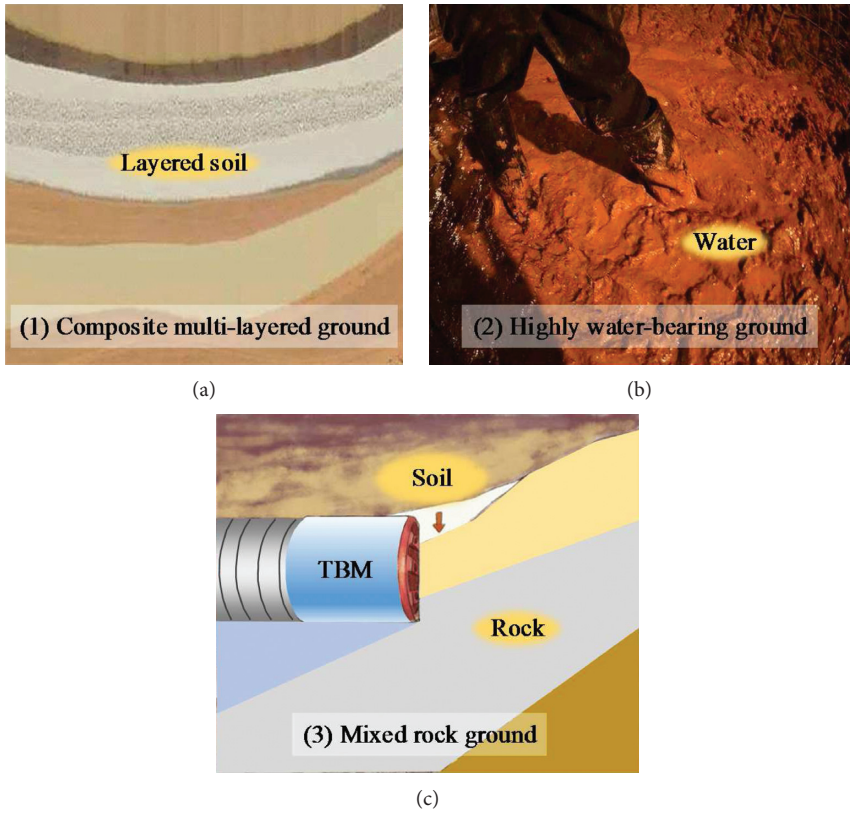

Figure 1: Three typical types of urban ground in China. (a) Composite multilayered ground, (b) highly water-bearing ground, and (c) mixed rock ground.

is always at the interface of soil and rock. This kind of ground has uneven soil properties, that is, soft soil at the top and hard rock at the bottom. The characteristic of this kind of ground is the soil-rock interface, and the interface has a great influence on ground movements. The main disasters are the failure of the soil-rock interface and soil slide.

The above three types of ground are the main types of urban ground in China. Among them, the proportion of composite multilayered ground is the largest, and the possibility of disaster is higher; therefore, this study focuses on this type of ground.

2.2. Ground Movement Prediction of Composite Multilayered Ground. Studies have shown that the settlement trough is much wider and shallower when tunnelling in clayey soils than that in sandy soils [46]. The difference is mainly caused by the deformation stiffness between different soil types on a macroscale [49]. The composite multilayered ground comprises several soil layers. The mechanical properties of each soil are different from others; therefore, the contribution of each soil layer to ground movements is different.

For composite multilayered ground with different mechanical properties, it is difficult to use traditional analytical methods to calculate ground movements. However, in view of the advantages of analytical methods, they can be used in case the multilayered soil system is transformed into the single soil layer system. A semianalytical method [46] (Figure 2) which can be used to calculate ground vertical displacements and transverse horizontal displacements has been proposed by combining the elastic equivalent theory [44] with the L & P formula [45].

In Figure 2, the left is the original multilayered soil system, and the right is the transformed single soil layer system. The transformation process is illustrated by Cao et al. [46]. The two soil systems are both plane strain models perpendicular to the tunnelling direction. The original coordinate system is the yOz system, y is horizontally to the right, and z is vertically downward. The transformed coordinate system is the $y'O'z'$ system, y' is horizontally to the right, and z' is vertically downward. The soil system comprises n layers, the tunnel crown is located at layer n_1, and the tunnel invert is located at layer n_2; therefore, the tunnel cross section covers $(n_2 - n_1 + 1)$ layers. i is the number of soil layers, and i is from 1 to n. H_i is the thickness of the ith layer in the original multilayered soil system. The displacements at tunnel opening are based on the double-circle [47] model with a distance of GAP at the tunnel crown. The GAP parameter is determined by the tunnelling operation parameters. This will be introduced in the following section. $\partial\Omega$ is the boundary of excavation, and $\partial\omega$ is the boundary of excavation after deformation at tunnel opening. $\partial\Omega'$ is the boundary of excavation by transformation, and $\partial\omega'$ is the boundary of excavation after deformation at tunnel opening by transformation. H_{ie} is the thickness of the ith layer in the transformed single soil layer system. ζ and η are arbitrary coordinate parameters within the

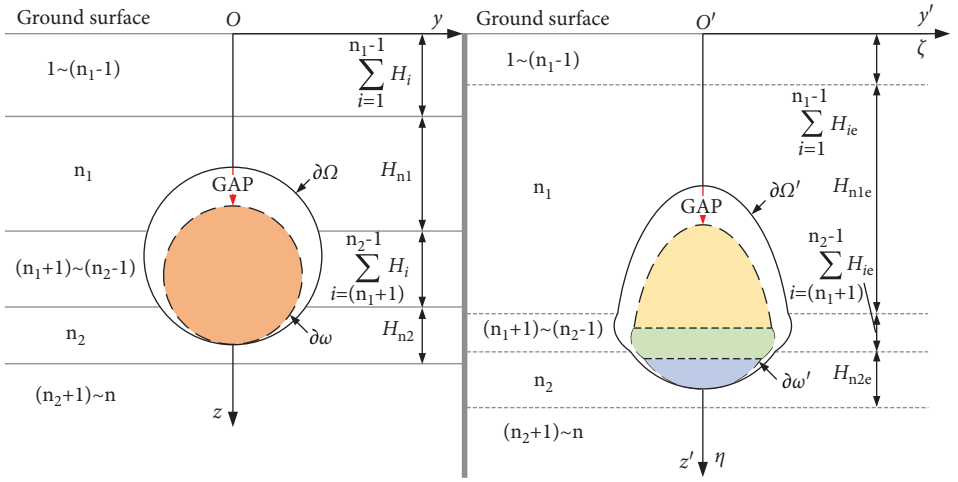

FIGURE 2: Transformation of the boundary of excavation $\partial\Omega$ and the boundary after convergence $\partial\omega$ from the multilayered soil system into the single layer soil system [46].

area which is enclosed by $\partial\Omega'$ and $\partial\omega'$. The direction of ζ and η are in accordance with y' and z', respectively.

According to the above regulations, the horizontal and vertical displacements of ground caused by tunnel tunnelling can be calculated by using the integral method in the following equation:

$$\left.\begin{aligned} S_{y\mathrm{Total}}(y,z) &= \iint_{\Omega'-\omega'} S_y(\zeta,\eta)\mathrm{d}\zeta\mathrm{d}\eta \\ S_{z\mathrm{Total}}(y,z) &= \iint_{\Omega'-\omega'} S_z(\zeta,\eta)\mathrm{d}\zeta\mathrm{d}\eta \end{aligned}\right\}, \tag{1}$$

where $S_{y\mathrm{Total}}(y,z)$ is the horizontal displacement caused by the tunnel excavation at the point (y,z), $S_{z\mathrm{Total}}(y,z)$ is the vertical displacement caused by the tunnel excavation at the point (y,z), Ω' is the enclosed area by $\partial\Omega'$, ω' is the enclosed area by $\partial\omega'$, $\mathrm{d}\zeta\mathrm{d}\eta$ is the unit area centered at the point (ζ,η) in the area enclosed by $\partial\Omega'$ and $\partial\omega'$ as the boundary, and $S_y(\zeta,\eta)$ and $S_z(\zeta,\eta)$ are the horizontal and vertical displacements at the point (y,z) caused by the excavation of unit area with the point (ζ,η) as the center. $S_y(\zeta,\eta)$ and $S_z(\zeta,\eta)$ contain GAP parameter (see [21] for specific expressions).

2.3. Effect of Tunnelling Parameters on Ground Movements. It can be seen from equation (1) that the ground displacements depend on the mechanical properties of each layer of soil on the one hand, and on the other hand, they mainly depend on the tunnelling parameters. For STM, the tunnelling parameters mainly include construction timing and stiffness of the shotcrete support and secondary lining. For SM, the tunnelling parameters include face pressure, grouting pressure, grouting volume, and attitude control parameters of TBM, among which face pressure and grouting volume may have an important influence on ground displacement. Whether it is STM or SM, the influence of tunnelling parameters on ground displacement is mainly reflected in the ground displacements at tunnel opening. The above-mentioned GAP parameter is often used to characterize this effect. The GAP parameter is defined as the maximum vertical displacement at tunnel crown [47], which is composed of 6 parts and can be expressed by the following equation [21]:

$$\begin{aligned} \mathrm{GAP} = {} & u_{3D}^{*} + G_{\mathrm{Physical}} + G_{\mathrm{Tapering}} + G_{\mathrm{Yawing}} \\ & + G_{\mathrm{Pitching}} - G_{\mathrm{Grouting}}, \end{aligned} \tag{2}$$

where GAP, u_{3D}^{*}, G_{Physical}, G_{Tapering}, G_{Yawing}, G_{Pitching}, and G_{Grouting} are the GAP parameter, the elastic-plastic vertical displacement at tunnel crown due to unbalanced force at tunnel face, gap needed to install lining, gap due to shield tapering, gap due to shield yawing, gap due to shield pitching, and gap due to shield grouting, respectively. In order to calculate each component, it is expressed in the form of equivalent diameter, as shown in Figure 3. The expressions are shown in the following equation:

$$\left.\begin{aligned} u_{3D}^{*} &= D_2 - D_1 \\ &= \frac{R(P_0 - P_s)}{2E_u} f\left(\frac{(P_0/k) - P_s}{c_u}\right) \\ G_{\mathrm{Physical}} &= D_1 - D_0 \\ G_{\mathrm{Tapering}} &= D_3 - D_2 = 2R - D_1 \\ G_{\mathrm{Yawing}} + G_{\mathrm{Pitching}} &= D_5 - D_3 \\ &= \min\left(0.6G_{\mathrm{Physical}}, \frac{u_{ps}}{3}\right) \\ G_{\mathrm{Grouting}} &= D_4 - D_0 \\ &= \sqrt{\frac{4V_{\mathrm{Grouting}}}{\pi l} + D_0^2} - D_0 \end{aligned}\right\}. \tag{3}$$

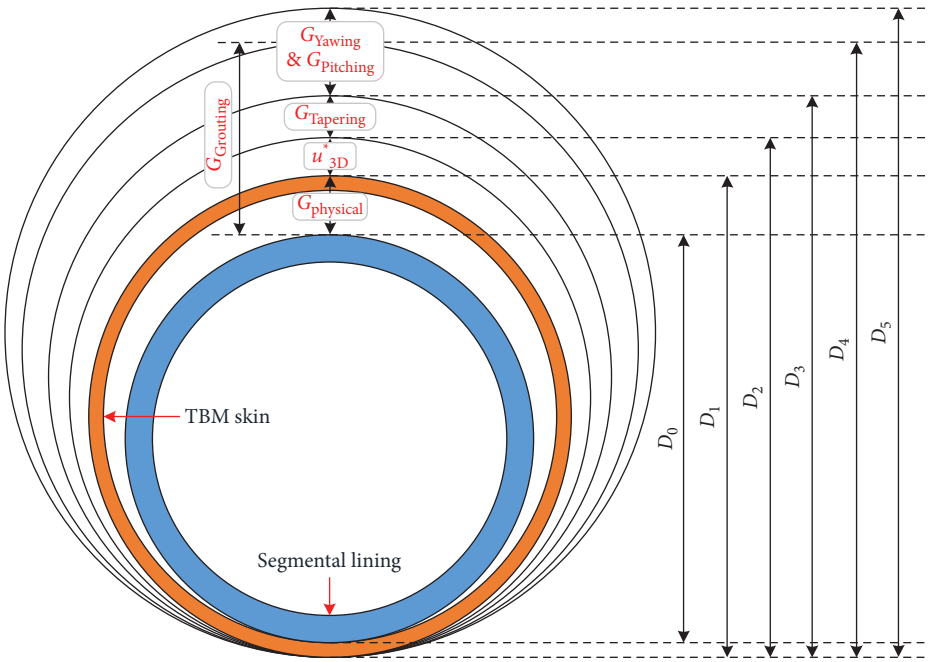

Figure 3: Schematic of equivalent diameter based on GAP parameter [46].

The meaning and calculation method of each parameter in equation (3) are illustrated in detail in [46]. Through the above analysis, combined with equations (1)–(3), the relationship between tunnelling parameters and ground displacement can be established.

3. Evolution of Environmental Disasters and Determination of Control Standards

Ground displacement at the tunnel opening occurs and then spreads to the environmental structures through the soil medium. The structures will deform even when the damage is caused by the interaction between soil and structures. When excessive ground displacement is produced, ground collapse will occur. Ground displacement is a key index to describe the evolution of the two disasters including ground collapse and structural failure. According to the displacement development stage of the soil and structures, corresponding displacement control standards can be established.

3.1. Evolution of the Ground Collapse. As the displacements at tunnel opening (GAP parameter) increase, the displacement within the ground increases subsequently. When the displacement increases to a certain extent, ground surface starts to generate cracks. With the further development of ground displacement, the fracture will propagate downward from the ground surface until a connected slip surface is formed (see the actual collapse boundary in Figure 4). According to the idea of Peck's theory [50], the horizontal strain ε_{zy} can be obtained by obtaining the partial derivative of the vertical displacement $S_{z\text{Total}}(y,z)$ in equation (1), as shown in the following equation:

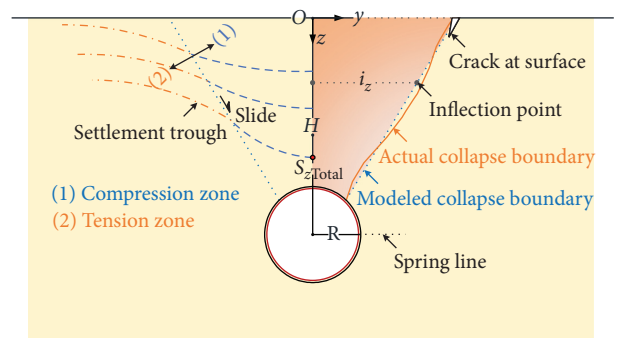

Figure 4: Schematic of ground collapse into tunnel opening.

$$\varepsilon_{zy} = \frac{\partial S_{z\text{Total}}(y,z)}{\partial y}. \tag{4}$$

When $y = i_z$, then $\varepsilon_{zy} = 0$, where i_z is the settlement trough width, z is the depth below ground surface, and y is the position of the inflection point. Within the inflection point of the settlement trough, the soil is subjected to compressive stress, which is the compression zone; outside the inflection point, the soil is subjected to tensile stress, which is the tension zone (Figure 4). Therefore, with the development of soil displacement, cracks are most likely to appear at the inflection point. The line of the inflection point at different soil depths is the potential slip surface (see the modeled collapse boundary in Figure 4).

Ground settlements undergo three typical stages with the increase of the GAP parameter, namely, the continuous deformation stage, the crack generation stage, and the collapse stage (Figure 5), which are as follows:

(1) During the continuous deformation stage, the structure mainly undergoes elastic deformation, and

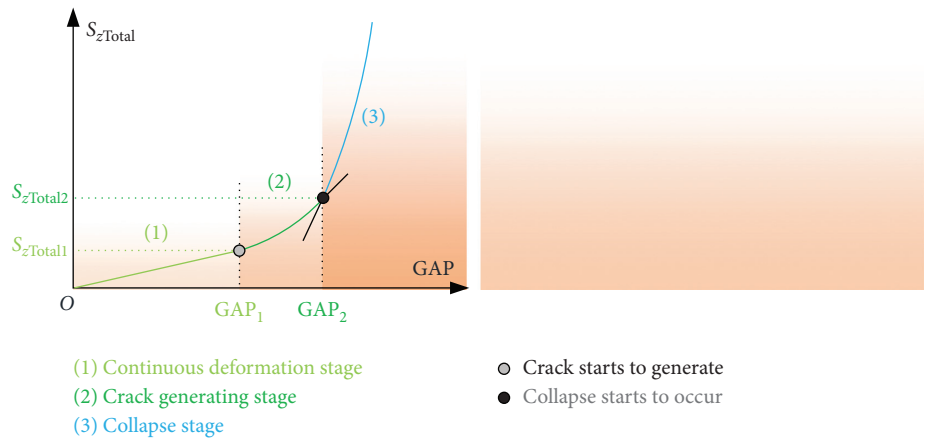

Figure 5: Ground displacements against GAP parameter (evolution of ground collapse).

the ground maximum settlements basically increase linearly with the increase of the GAP parameter

(2) During the crack generation stage, the soil begins to deform discontinuously, and cracks occur, and the ground settlements show a nonlinear increasing trend as the GAP parameter continues to increase

(3) During the collapse stage, the slight increase of the GAP parameter leads to a significant increase in ground settlements, and due to the penetration of the cracks, the appearance of the slip surface marks the formation of the ground collapse disaster

3.2. Evolution of the Structural Failure. Ground deformation caused by tunnelling propagates to the environmental structures; then, the structures start to deform subsequently. When the structural internal force exceeds the strength of the structures, the structure will be damaged [25]. Existing structures include ground surface structures such as road and building (Figure 6), underground structures such as subway and pipeline (Figure 7), and pile foundation (Figure 8).

These environmental structures can be divided into three types from their load characteristics. The road structure and the building structure belong to the first type (Figure 6). The characteristic is that the structure is not all placed in the soil, showing the load characteristics of both ground surface structures and underground structures. The second type is the subway structure and pipeline (Figure 7), which is characterized by all the structures that are within the soil and are placed horizontally. The characteristic of these structures is that they are mainly subjected to vertical soil loads, and the distribution of soil loads is generally continuous. The third type is the pile including single pile and pile group (Figure 8), which is also characterized by all being placed in the soil. Different from the second type, the soil load on this type of structure is mainly horizontal. Since the structure spans different soil layers from top to bottom, the soil load on the structure is often discontinuous.

Regardless of the type of structures, a simplified method which is called the two-stage method (TSM) can be used to predict and evaluate the deformation of the structures. Because the TSM mentioned in the current paper is mainly based on the elastic beam which is the object in the

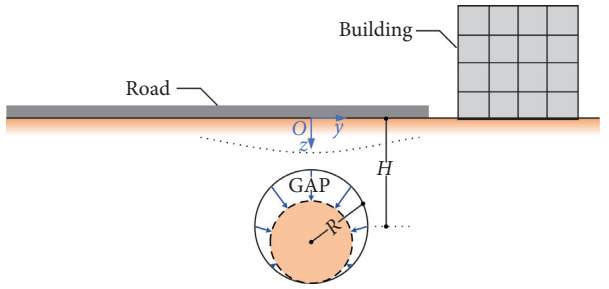

Figure 6: Road and building.

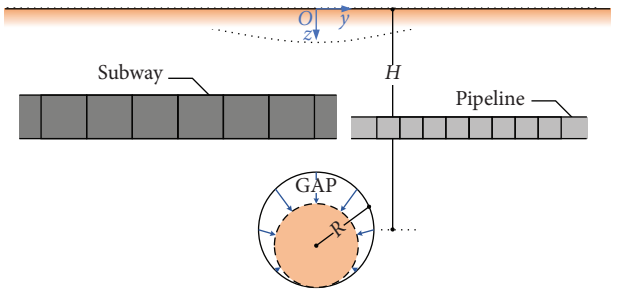

Figure 7: Subway and pipeline.

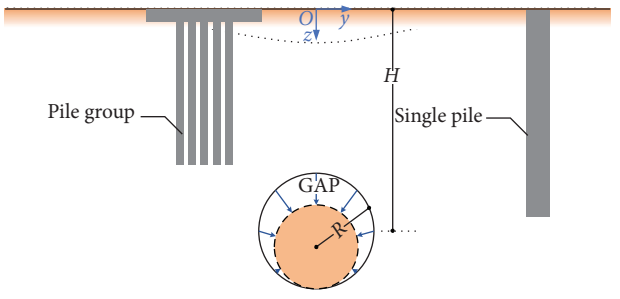

Figure 8: Single pile and pile group.

mechanics of materials. When applying this method, the dimension of the structure under consideration in its extension direction should be much larger than that in the other two directions, such as piles, existing lines, and pavements. If this condition is not met, the error of the solution will be very large. In this case, the theory of elasticity must be used to solve the problem. The steps of TSM are as follows: (1) the ground displacements are calculated without considering the existence of the structures; (2) the structures are simplified to an elastic beam model placed on the soil foundation model; (3) the ground displacements are applied to the beam model, and (4) finally, the deformation and internal force of the structures are obtained. Beam models usually include Euler–Bernoulli beam and Timoshenko beam, and foundation models usually include the Winkler model, Pasternak model, and Kerr model (Figure 9).

Among them, the governing differential equation of the Euler–Bernoulli beam model on the Pasternak foundation model, which is widely used, can be expressed by the following equation [30]:

$$EI\frac{\mathrm{d}^4 w}{\mathrm{d}\psi^4} - GD\frac{\mathrm{d}^2 w}{\mathrm{d}\psi^2} + kDw = pD, \tag{5}$$

where E is the elastic modulus of the structure; I is the moment of inertia of the structure; D is the equivalent thickness perpendicular to the extension direction of the structure; G is the stiffness of the shear layer per unit thickness of the foundation; k is the stiffness of the spring; p is the additional load applied on the structure; w is the displacements of the structure perpendicular to the extension direction; and ψ is the coordinate along the extension direction of the structure (any direction of x, y, and$z$). Among them, k, G, and p can be expressed as

$$\begin{cases} k = \dfrac{0.65}{D}\left(\dfrac{E_s D^4}{EI}\right)^{\dfrac{1}{12}}\dfrac{E_s}{1-\mu_s^2}, \\ G = \dfrac{E_s t}{6(1+\mu_s)}, \\ p = kS - G\dfrac{\mathrm{d}^2 S}{\mathrm{d}\psi^2}, \end{cases} \tag{6}$$

where E_s and μ_s are the elastic modulus and Poisson's ratio of the soil; t is the thickness of the shear layer; and S is the greenfield displacements of the soil perpendicular to the extension direction of the structure, which can be calculated by equation (1).

In view of the nonlinearity of the differential equation (5), it is usually solved by the differential method. The displacements of the structure perpendicular to the extension direction at different positions can be calculated, and the bending moment and stress of the structure can be further determined, as shown in the following equation:

$$\begin{cases} M = EI\dfrac{\mathrm{d}^2 w}{\mathrm{d}\psi^2} \\ \sigma = \dfrac{M\phi}{\mathrm{I}} \\ \sigma_{\max} \le [\sigma] \end{cases}, \tag{7}$$

where M is the bending moment of the structure; σ is the bending stress of the structure; $\sigma_{\max}$ is the maximum bending stress of the structure; $[\sigma]$ is the strength of the structure; and ϕ is the distance of the boundary from the neutral axis (vertical to the coordinate direction ψ).

When the maximum stress reaches the strength of the structure, the structure starts to be destroyed. The development process of structural deformation is in accordance with the incubation process of structural failure, which is similar to the ground collapse (Figure 5). The process can be also divided into three stages including the continuous deformation stage, the failure development stage, and the total failure stage (Figure 10), which are as follows:

(1) During the continuous deformation stage, the structure is mainly elastic deformation, and the deformation of the structure basically increases linearly with the increase of the GAP parameter.

(2) During the failure development stage, the maximum bending stress of the structure reaches the material strength, and local failure begins to occur. Therefore, the deformation of the structure shows a nonlinear increasing trend as the GAP parameter continues to increase.

(3) During the total failure stage, the stresses at the most vulnerable interface of the structure all reach the material strength, the structure is completely destroyed, and the disaster is officially formed.

Overall, both disasters including ground collapse and structural failure are characterized by ground deformation, and the development of ground displacement is equivalent to the evolution of the disasters. Therefore, grasping the development of ground displacement and formulating corresponding control standards are key issues to ensure safety during tunnelling.

3.3. Determination of the Displacement Control Standards. According to the above research, when the displacement of the ground and the structure begins to enter the second stage, cracks begin to occur, and the structure begins to undergo local damage. Therefore, it should be ensured that the displacement is within the first stage during tunnelling. Naturally, the changing point ($S_{z\mathrm{Total1}}$ in Figure 5 and w_1 in Figure 10) between the first stage and the second stage is the preliminary displacement control standard. However, in actual engineering, there are certain existing displacements in the ground (L_{G}) and the structure (L_{S}) before the tunnel excavation. At the same time, the ground usually has defects, and the existing structure is also degraded and damaged due

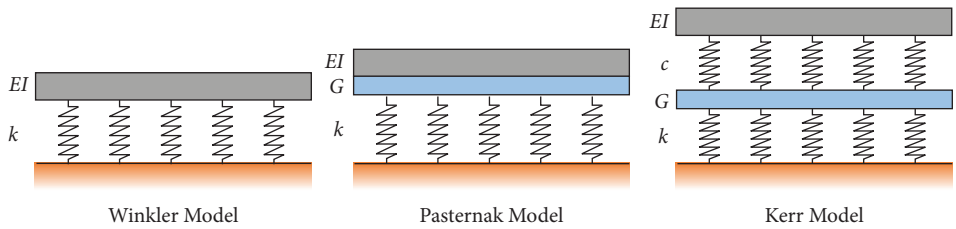

Figure 9: Three typical foundations in structure-soil interaction analysis. (a) Winkler model, (b) Pasternak model, and (c) Kerr model.

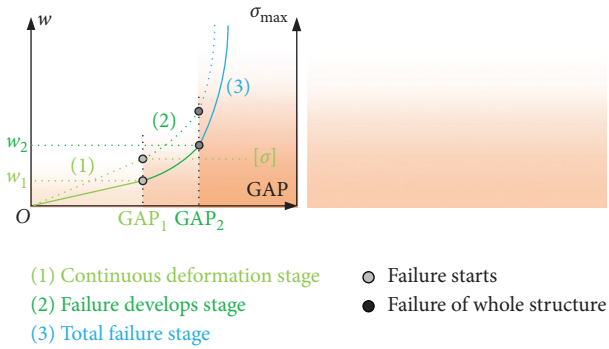

Figure 10: Displacements of environmental structures against GAP parameter (evolution of structural failure).

to the increase in service life. Therefore, it is necessary to consider the above two factors (existing displacement and degraded) on the basis of the preliminary displacement control standards ($S_{z\text{Total1}}$ and w_1). Furthermore, considering the safety, the safety factors (ω_G and ω_S) should be introduced to reduce the displacement control standards to a certain extent. By considering the above factors, the displacement control standards that can be adopted in the tunnelling process are finally obtained, as shown in the following equation:

$$\begin{cases} [L_G] = \dfrac{\chi_G (S_{z\,\text{Total1}} - L_G)}{\omega_G}, \\ [L_S] = \dfrac{\chi_S (w_1 - L_S)}{\omega_S}, \end{cases} \tag{8}$$

where L_G is the existing displacements of the ground; L_S is the existing displacements of the environmental structure; χ_G is the reduction coefficient of the ground considering the defects within the ground ($0 < \chi_G \leq 1$); χ_S is the reduction coefficient of the structure considering the damage and deterioration characteristics of the structure due to the increase in service life ($0 < \chi_S \leq 1$); ω_G is the safety factor of the ground ($\omega_G \geq 1$); ω_S is the safety factor of the structures ($\omega_S \geq 1$); $[L_G]$ is the final displacement control standard of the ground; and $[L_S]$ is the final displacement control standard of structures.

4. Framework of Displacement Control during Tunnelling Process

The fundamental purpose of the displacement prediction and the formulation of displacement control standards for the built environment is the controllable safety of the tunnelling process. In view of the complexity of the soil conditions and the uncertainty of the tunnelling, the prediction of displacement and the selection of tunnelling parameters must be adjusted and updated during the construction process. In-time monitoring of the displacements of the ground and existing structures during the tunnelling provides a direct way to capture the safety status of the ground and structures. It is also a crucial way to correct the prediction method and adjust the tunnelling parameters based on the feedback analysis [43]. During the tunnelling process, the in-process control theory links the monitoring data with the prediction method and directly feeds back the tunnelling parameters.

4.1. Theoretical Framework of In-Process Control. Before tunnelling, preliminary tunnelling parameters can be specified based on geological conditions and dimensions of the bored tunnel. During the tunnelling process, the tunnelling parameters can be modified. Firstly, the prediction method is modified according to the monitoring data step by step. Then, based on the modified prediction method, the tunnelling parameters can be modified provided that the newly produced displacement of ground and structures meets the displacement control standard.

Taking shield construction as an example, it contains m tunnelling parameters (face pressure, grouting pressure, etc.) and n ring bored distance. Matrix $\mathbf{P}$ is the tunnelling parameter matrix, which is a matrix with n rows and m columns:

$$\mathbf{P} = \begin{pmatrix} p_{11} & p_{21} & \cdots & p_{j1} & \cdots & p_{m1} \\ p_{12} & p_{22} & \cdots & p_{j2} & \cdots & p_{m2} \\ \vdots & \vdots & \vdots & \vdots & \vdots & \vdots \\ p_{1i} & p_{2i} & \cdots & p_{ji} & \cdots & p_{mi} \\ \vdots & \vdots & \vdots & \vdots & \vdots & \vdots \\ p_{1n} & p_{2n} & \cdots & p_{jn} & \cdots & p_{mn} \end{pmatrix}, \tag{9}$$

where p_{ji} is the value of j th tunnelling parameter in i th tunnelling step ($1 \leq j \leq m$, $1 \leq i \leq n$). The displacements of ground or structure after i th tunnelling step F_i can be calculated based on equations (1)–(3) and (5)-(6). These equations are the prediction model and can be written as $f_i()$ for the convenience of expression shown in the following equation:

$$F_i = f_i(P_i). \tag{10}$$

In fact, because of the unpredictability of the ground conditions and the uncertainty of the parameters in the prediction model $f_i()$, it also needs to be updated in time to ensure the accuracy of the displacement prediction. These updates can be accomplished by the matrix $\mathbf{X}$, which includes l ground mechanical parameters and other coefficients in the prediction model $f_i()$. The matrix $\mathbf{X}$ is shown in the following equation:

$$\mathbf{X} = \begin{pmatrix} x_{11} & x_{21} & \cdots & x_{j1} & \cdots & x_{l1} \\ x_{12} & x_{22} & \cdots & x_{j2} & \cdots & x_{l2} \\ \vdots & \vdots & \vdots & \vdots & \vdots & \vdots \\ x_{1i} & x_{2i} & \cdots & x_{ji} & \cdots & x_{li} \\ \vdots & \vdots & \vdots & \vdots & \vdots & \vdots \\ x_{1n} & x_{2n} & \cdots & x_{jn} & \cdots & x_{ln} \end{pmatrix}, \tag{11}$$

where x_{ji} is the value of j th coefficient in i th prediction model $f_i()$ $(1 \le j \le l\ ,\ 1 \le i \le n\ )$. Based on the back analysis, the value of each element in the matrix $\mathbf{X}$ can be calculated given that the monitoring data are obtained. The objective function is $\Phi(\mathrm{X}_i)$ and shown in the following equation:

$$\Phi(\mathbf{X}_i) = \left(\frac{(F_i - F_{i-1}) - (S_i - S_{i-1})}{(S_i - S_{i-1})} \right)^2, \tag{12}$$

where S_i is the measured displacements of ground or environmental structures after i th tunnelling step. Based on the least square method, the coefficients of the prediction model $f_i()$ can be calculated using the following equation:

$$\min \Phi(X_i). \tag{13}$$

After X_i is obtained, the prediction model $f_i()$ is updated to $f_{i+1}()$, which will be used to calculate the tunnelling parameters of the $(i+1)$ th step given that the following equation holds

$$\left(F_{i+1} + \sum_{j=1}^{i} S_j \right) \le \sum_{j=1}^{i+1} [L], \tag{14}$$

where $[L]$ is the displacement control standard, and it is $[L_G]$ for the ground and $[L_S]$ for the structure; F_{i+1} is the displacements of ground or environmental structures after $(i+1)$ th tunnelling step, $F_{i+1} = f_{i+1}(\mathbf{P}_{i+1})$. Based on equation (14), the $(i+1)$ th tunnelling parameters $\mathbf{P}_{i+1}$ can be recommended and updated.

4.2. Overview of the Qinghuayuan Tunnel Project. Qinghuayuan Tunnel is a part of the Beijing–Zhangjiakou High-Speed Railway, which is excavated using an SPB TBM with the cutterhead diameter of 12.64 m. The external and internal diameters of the tunnel are 12.2 m and 11.1 m, respectively. Other specific information can be found in [21]. The tunnel passes the running tunnel of Beijing Subway Line 10 below with a clearance of about 6.5 m; besides, there is an existing Zhichun Road directly above the running tunnel. The transverse and longitudinal profiles of the layout are shown in Figure 11.

The ground is mainly composed of backfill, silt, silty clay I, gravel, silty clay II, and silty sand from the surface to the deep of the ground (Figure 11). The mechanical properties of each soil are illustrated in Table 1. The upper section of the Qinghuayuan Tunnel is located in gravel, and a small part of the lower section is located in silty clay and silt sand. Drilling revealed that the buried depth of the water level of the aquifer is between 1.38 m and 5.09 m below the ground surface. The aquifer is mainly located in silt and silt sand, which mainly receives atmospheric precipitation recharge, followed by pipeline leakage recharge.

As the newly built tunnel passes through the existing twin tunnel with a close clearance, ground displacement caused by the tunnel tunnelling will inevitably affect the existing tunnels, which will result in the suspension of the subway and even the destruction of the subway structure. In order to ensure the safety of the structure, two vertical shafts were constructed on the north and south sides of the existing tunnel (Figure 11). The construction staff and equipment were lowered to the top of the new tunnel through the shaft, and the soil between the tunnels was reinforced by grouting with multilayered small pipes. The developed stiff grouting structure can protect the two tunnels from destruction. In order to obtain the safety status of the existing tunnel, settlement measured points are arranged at the center of the tunnel invert (Figure 11).

4.3. Application of the In-Process Control. According to the geological conditions, the preliminary tunnelling parameters were selected for tunnelling. Then, the settlement control standard of the subway structure was determined to be 3.00 mm considering the safety. Because the settlements of the structure gradually increase with the tunnelling process, the accumulated settlements may increase sharply at a certain tunnelling stage. If the settlements of the structure are controlled only by the total control standard, accidents occur easily. Therefore, the total control standard should be decomposed into each tunnelling stage, and the control standard of each stage should be established. During construction, it is necessary to ensure that after a certain stage of tunnelling, the cumulative settlements of the structure are less than the control standard of the current stage. This is the most important feature of the in-process control.

In the current project, the tunnelling process is divided into four main stages including (1) TBM approaching, (2) TBM passing, (3) grouting and void closure, and (4) consolidation and ovalization (Figure 12).

The control standards after stage 1, stage 2, stage 3, and stage 4 are 0.5 mm, 2.00 mm, 2.75 mm, and 3.00 mm, respectively. The measured results of the monitoring point installed at the tunnel invert (blue point in Figure 11) and four-time settlement prediction are shown in Figure 12. The predictions are modified based on the in-process measurements, which are all within the control standards of each stage (noted that, before these four predictions, there was another prediction that did not consider protecting

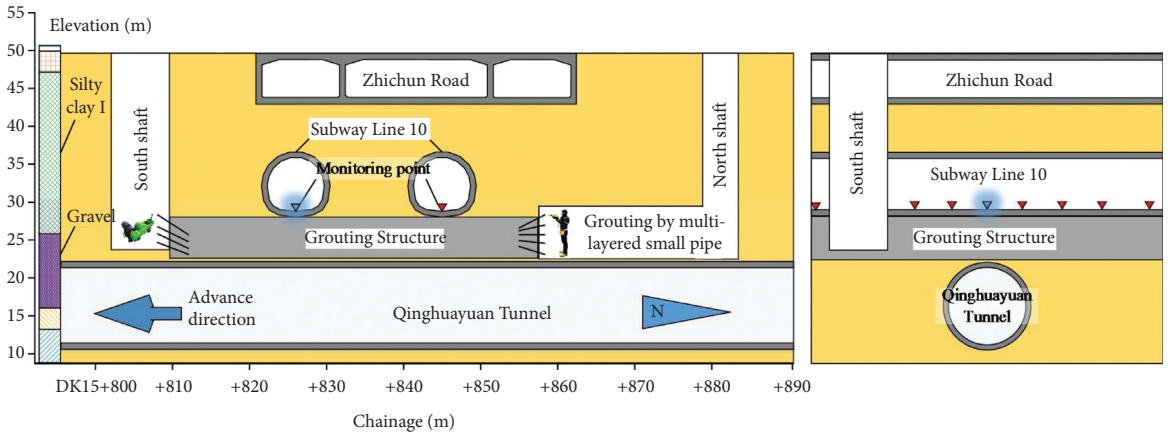

Figure 11: Longitudinal and transverse profile of the Qinghuayuan Tunnel Project.

Table 1: Physical and mechanical properties of soils.

Soil type	Specific weight (kN/m^3)	Elastic modulus (MPa)	Poisson's ratio	Cohesion (KPa)	Internal friction (°)
Backfill	16.60	8.20	0.34	4.90	24.50
Silt	19.90	10.10	0.31	24.30	25.20
Silty clay I	19.80	26.50	0.28	33.57	18.10
Gravel	18.90	44.60	0.22	0	39.80
Silty clay II	20.10	27.00	0.30	33.80	18.40
Silt sand	20.40	27.30	0.27	0.10	33.50

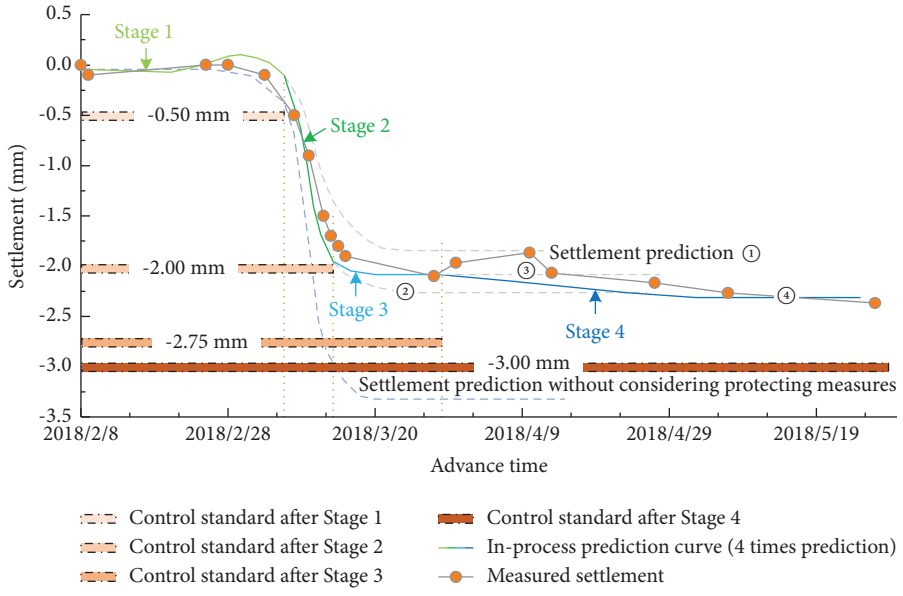

Figure 12: In-process control of tunnelling-induced displacements.

measures). The modification of the prediction model and corresponding parameters improves the accuracy of settlement prediction so as to the adjustment of the tunnelling parameters. The in-process tunnelling parameters including trust, advance rate, torque, rotation rate, grouting pressure, and grouting volume are shown in Figure 13. The adjustment of these parameters is based on the feedback of the measured data. Before the shield reaches the existing subway structure, the structure heaves slightly according to the feedback of the monitoring data, in order to prevent uneven heave of the structure due to excessive tunnelling parameters, which are adjusted to be at a low level.

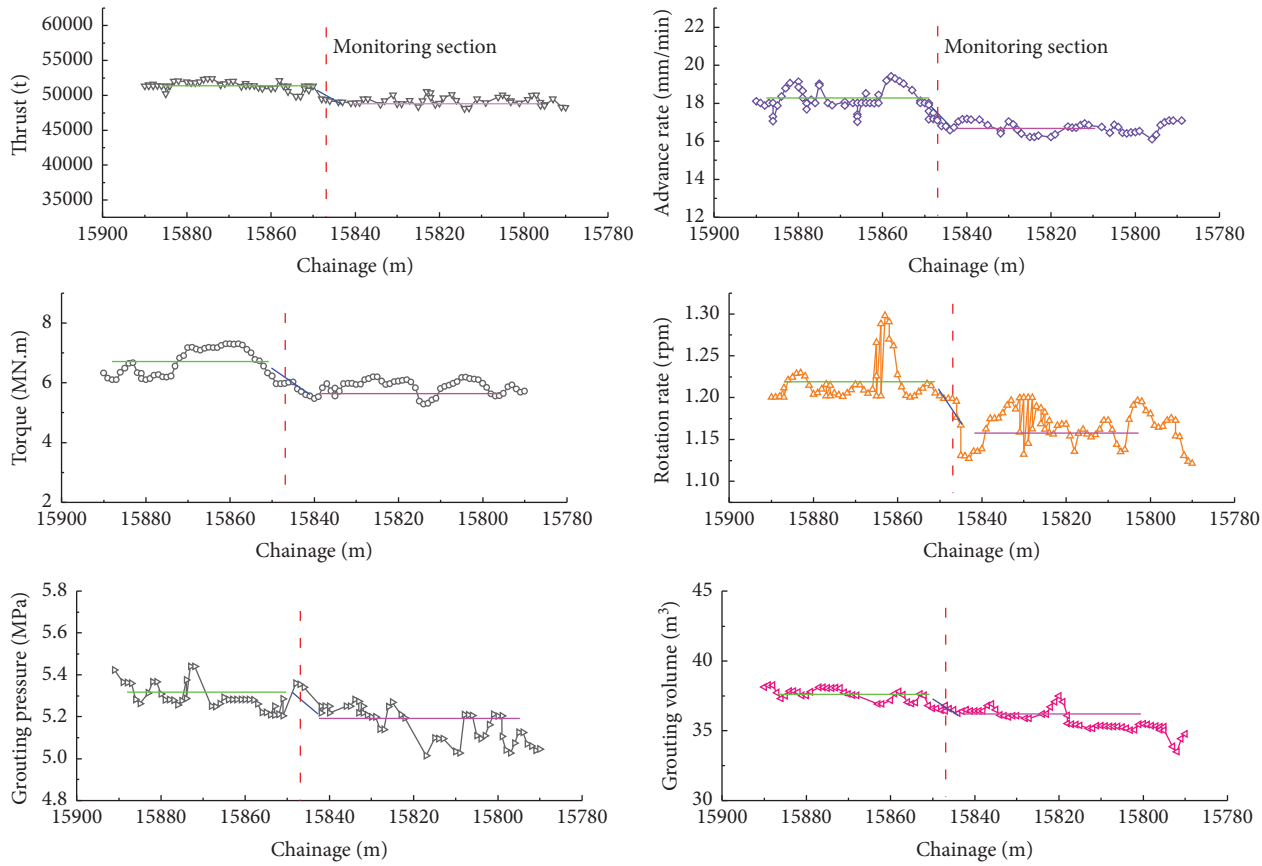

Figure 13: Adjustment of tunnelling parameters during the construction process.

5. Conclusions

The environmental responses induced by tunnelling including ground movements and deformation of the environmental structures are the prominent issues needed to be carefully disposed during tunnel construction in urban areas. This paper tries to develop a theoretical framework to evaluate and control these environmental displacements to avoid two disasters including ground collapse and structural failure, and the framework is successfully applied in the Qinghuayuan Tunnel Project. Meanwhile, some major conclusions are drawn as follows:

(1) According to the mechanical responses of the ground due to tunnelling, the urban ground in China can be roughly divided into three types including composite multilayered ground, highly water-bearing ground, and mixed rock ground. The main disasters of composite multilayered ground are the ground collapse and the failure of the environmental structures due to excessive ground displacements. The main disasters of the highly water-bearing ground are the water inrush during the excavation process and the long-term displacements due to consolidation. The main disasters of the mixed rock ground are the failure of the soil-rock interface and soil slide.

(2) The displacements of ground and existing structures due to tunnelling in the multilayered ground are emphatically discussed in view of its largest proportion distribution. The cumulative and mutational characteristics of the displacement are considered, which can be the main basis for distinguishing the occurrence of two types of disasters including ground collapse and structural failure; thus, the three-stage evolution model of disaster can be established based on the development of the displacements. Based on the influence of tunnelling parameters on ground displacements, the quantitative relationship between tunnelling parameters and the evolution of disasters can be further determined.

(3) Based on the evolution of the disasters, combined with the existing displacement and degeneration of ground and environmental structures and the safety factor, the displacement control standards can be eventually determined. The total control standards should be decomposed into each tunnelling stage avoiding a sharp increase in accumulated settlements. The theoretical framework of in-process control is proposed which is based on the prediction, measurement, and control standards of the displacements. The prediction model can be modified in time, and the tunnelling parameters can be adjusted synchronously. The in-process control framework is

successfully applied in the Qinghuayuan Tunnel Project.

Data Availability

The data used to support the findings of this study are unavailable due to the legal and ethical concerns.

Conflicts of Interest

The authors declare that they have no conflicts of interest.

Acknowledgments

The authors gratefully acknowledge the financial support by the National Natural Science Foundation of China (Grant nos. 52108376, 51738002, and 51938008) and Open Project Foundation of the Key Laboratory of Urban Underground Engineering of Ministry of Education (Beijing Jiaotong University) (Grant no. TUL2020-03).

References

[1] W. Broere and D. Festa, "Correlation between the kinematics of a Tunnel Boring Machine and the observed soil displacements," *Tunnelling and Underground Space Technology*, vol. 70, pp. 125–147, 2017.

[2] M. Zhu, X. N. Gong, X. Gao, S. Liu, and J Yan, "Remediation of damaged shield tunnel using grouting technique: serviceability improvements and prevention of potential risks," *Journal of Performance of Constructed Facilities*, vol. 33, no. 6, Article ID 04019062, 2019.

[3] L. Cao, Q. Fang, D. Zhang, and T. Chen, "Subway station construction using combined shield and shallow tunnelling method: case study of Gaojiayuan station in Beijing," *Tunnelling and Underground Space Technology*, vol. 82, pp. 627–635, 2018.

[4] D. Jin, X. Shen, and D. Yuan, "Theoretical analysis of three-dimensional ground displacements induced by shield tunneling," *Applied Mathematical Modelling*, vol. 79, pp. 85–105, 2020.

[5] Q. Fang, J. M. Du, J. Y. Li, D. l Zhang, and L. Q Cao, "Settlement characteristics of large-diameter shield excavation below existing subway in close vicinity," *Journal of Central South University*, vol. 28, pp. 882–897, 2021.

[6] P. F. Li, K. Y. Chen, F. Wang, and Z Li, "An upper-bound analytical model of blow-out for a shallow tunnel in sand considering the partial failure within the face," *Tunnelling and Underground Space Technology*, vol. 91, Article ID 102989, 2019.

[7] W. Li and C. P. Zhang, "Face stability analysis for a shield tunnel in anisotropic sands," *International Journal of Geomechanics*, vol. 20, no. 5, Article ID 04020043, 2020.

[8] X. T. Lin, R. P. Chen, H. N. Wu, and H. Z Cheng, "Three-dimensional stress-transfer mechanism and soil arching evolution induced by shield tunneling in sandy ground," *Tunnelling and Underground Space Technology*, vol. 93, Article ID 103104, 2019.

[9] L. Tao, P. Ding, X. R. Yang et al., "Comparative study of the seismic performance of prefabricated and cast-in-place subway station structures by shaking table test," *Tunnelling and Underground Space Technology*, vol. 105, Article ID 103583, 2020.

[10] J. Liu, C. Shi, M. Lei, C. Cao, and Y Lin, "Improved analytical method for evaluating the responses of a shield tunnel to adjacent excavations and its application," *Tunnelling and Underground Space Technology*, vol. 98, Article ID 103339, 2020.

[11] X. N. Rong, H. Lu, M. Y. Wang, Z. Wen, and X Rong, "Cutter wear evaluation from operational parameters in EPB tunneling of Chengdu Metro," *Tunnelling and Underground Space Technology*, vol. 93, Article ID 103043, 2019.

[12] C. J. Gong, W. Q. Ding, and D. W. Xie, "Twin EPB tunneling-induced deformation and assessment of a historical masonry building on Shanghai soft clay," *Tunnelling and Underground Space Technology*, vol. 98, Article ID 103300, 2020.

[13] E. Ieronymaki, A. J. Whittle, and H. H. Einstein, "Comparative study of the effects of three tunneling methods on ground movements in stiff clay," *Tunnelling and Underground Space Technology*, vol. 74, pp. 167–177, 2018.

[14] Q. Fang, G. Wang, F. Yu, and J Du, "Analytical algorithm for longitudinal deformation profile of a deep tunnel," *Journal of Rock Mechanics and Geotechnical Engineering*, vol. 13, pp. 845–854, 2021.

[15] Q. Fang, D. L. Zhang, and L. N. Y. Wong, "Shallow tunnelling method (STM) for subway station construction in soft ground," *Tunnelling and Underground Space Technology*, vol. 29, pp. 10–30, 2012.

[16] A. Morovatdar, M. Palassi, and R. S. Ashtiani, "Effect of pipe characteristics in umbrella arch method on controlling tunneling-induced settlements in soft grounds," *Journal of Rock Mechanics and Geotechnical Engineering*, vol. 12, pp. 984–1000, 2020.

[17] M. N. Vu and W. Broere, "Structural design model for tunnels in soft soils: from construction stages to the long-term," *Tunnelling and Underground Space Technology*, vol. 78, pp. 16–26, 2018.

[18] Y. Liang, X. Chen, J. Yang, J. Zhang, and L. Huang, "Analysis of ground collapse caused by shield tunnelling and the evaluation of the reinforcement effect on a sand stratum," *Tunnelling and Underground Space Technology*, vol. 115, Article ID 104616, 2020.

[19] Y. L. Zheng, Q. B. Zhang, and J. Zhao, "Challenges and opportunities of using tunnel boring machines in mining," *Tunnelling and Underground Space Technology*, vol. 57, pp. 287–299, 2016.

[20] J. Z. Huo, Z. H. Xu, Z. C. Meng, J. Li, J. Dong, and L Wang, "Coupled modeling and dynamic characteristics of TBM cutterhead system under uncertain factors," *Mechanical Systems and Signal Processing*, vol. 140, Article ID 106664, 2020.

[21] L. Q. Cao, D. L. Zhang, Q. Fang, and L Yu, "Movements of ground and existing structures induced by slurry pressure-balance tunnel boring machine (SPB TBM) tunnelling in clay," *Tunnelling and Underground Space Technology*, vol. 97, Article ID 103278, 2020.

[22] A. Mahmoodzadeh, M. Mohammadi, A. Daraei, H. F. H Ali, N. k. A Salihi, and R. M, D Omer, "Forecasting maximum surface settlement caused by urban tunneling," *Automation in Construction*, vol. 120, Article ID 103375, 2020.

[23] C. P. Zhang, K. H. Han, and D. L. Zhang, "Face stability analysis of shallow circular tunnels in cohesive–frictional soils," *Tunnelling and Underground Space Technology*, vol. 50, pp. 345–357, 2015.

[24] C. P. Zhang, W. Li, W. J. Zhu, and Z Tan, "Face stability analysis of a shallow horseshoe-shaped shield tunnel in clay with a linearly increasing shear strength with depth,"

Tunnelling and Underground Space Technology, vol. 97, Article ID 103291, 2020.

[25] D. L. Zhang, Q. Fang, Y. J. Hou, P. Li, and L. N Wong, "Protection of buildings against damages as a result of adjacent large-span tunneling in shallowly buried soft ground," *Journal of Geotechnical and Geoenvironmental Engineering*, vol. 139, no. 6, pp. 903–913, 2013.

[26] B. T. Cao, M. Obel, S. Freitag, and P. Mark, G Meschke, Artificial neural network surrogate modelling for real-time predictions and control of building damage during mechanised tunneling," *Advances in Engineering Software*, vol. 149, Article ID 102869, 2020.

[27] F. C. Kong, D. C. Lu, X. L. Du, and C Shen, "Elastic analytical solution of shallow tunnel owing to twin tunnelling based on a unified displacement function," *Applied Mathematical Modelling*, vol. 68, pp. 422–442, 2019.

[28] A. Franza and A. M. Marshall, "Empirical and semi-analytical methods for evaluating tunnelling-induced ground movements in sands," *Tunnelling and Underground Space Technology*, vol. 88, pp. 47–62, 2019.

[29] D. C. Lu, Q. T. Lin, Y. Tian, X. Du, and Q Gong, "Formula for predicting ground settlement induced by tunnelling based on Gaussian function," *Tunnelling and Underground Space Technology*, vol. 103, Article ID 103443, 2020.

[30] Z. G. Zhang, M. S. Huang, C. Xu, Y. Jiang, and W Wang, "Simplified solution for tunnel-soil-pile interaction in Pasternak's foundation model," *Tunnelling and Underground Space Technology*, vol. 78, pp. 146–158, 2018.

[31] A. Franza, S. Acikgoz, and M. J. DeJong, "Timoshenko beam models for the coupled analysis of building response to tunnelling," *Tunnelling and Underground Space Technology*, vol. 96, Article ID 103160, 2020.

[32] M. A. Soomro, N. Mangi, H. Xiong, M. Kumar, and D. A Mangnejo, "Centrifuge and numerical modelling of stress transfer mechanisms and settlement of pile group due to twin stacked tunnelling with different construction sequences," *Tunnelling and Underground Space Technology*, vol. 121, Article ID 103449, 2020.

[33] P. F. Li, F. Wang, C. P. Zhang, and Z Li, "Face stability analysis of a shallow tunnel in the saturated and multilayered soils in short-term condition," *Computers and Geotechnics*, vol. 107, pp. 25–35, 2019.

[34] L. Yu, D. L. Zhang, Q. Fang, L. Cao, Y. Zhang, and T Xu, "Face stability of shallow tunnelling in sandy soil considering unsupported length," *Tunnelling and Underground Space Technology*, vol. 102, Article ID 103445, 2020.

[35] P. F. Li, H. H. Zou, F. Wang, and H. C Xiong, "An analytical mechanism of limit support pressure on cutting face for deep tunnels in the sand," *Computers and Geotechnics*, vol. 119, Article ID 103372, 2020.

[36] P. F. Li, Y. F. Wei, M. J. Zhang, Q. F. Huang, and F. Wang, "Influence of non-associated flow rule on passive face instability for shallow shield tunnels," *Tunnelling and Underground Space Technology*, vol. 119, Article ID 104202, 2022.

[37] M. J. Zhang, Q. G. Di, P. F. Li, Y. J. Wei, and F. Wang, "Influence of non-associated flow rule on face stability for tunnels in cohesive–frictional soils," *Tunnelling and Underground Space Technology*, vol. 121, Article ID 104320, 2022.

[38] G. Zheng, T. Cui, X. Cheng et al., "Study of the collapse mechanism of shield tunnels due to the failure of segments in sandy ground," *Engineering Failure Analysis*, vol. 79, pp. 464–490, 2017.

[39] R. Li, D. L. Zhang, Q. Fang, D. Liu, J. Luo, and H Fang, "Mechanical responses of closely spaced large span triple tunnels," *Tunnelling and Underground Space Technology*, vol. 105, Article ID 103574, 2020.

[40] G. W. Xu, C. He, Z. Q. Chen, C. Liu, B. Wang, and Y Zou, "Mechanical behavior of secondary tunnel lining with longitudinal crack," *Engineering Failure Analysis*, vol. 113, Article ID 104543, 2020.

[41] L. Y. Ding and C. Zhou, "Development of web-based system for safety risk early warning in urban metro construction," *Automation in Construction*, vol. 34, pp. 45–55, 2013.

[42] X. J. Li and H. H. Zhu, "Development of a web-based information system for shield tunnel construction projects," *Tunnelling and Underground Space Technology*, vol. 37, pp. 146–156, 2013.

[43] X. Y. Xie, Q. Wang, I. Shahrour, J. Li, and B Zhou, "A real-time interaction platform for settlement control during shield tunnelling construction," *Automation in Construction*, vol. 94, pp. 154–167, 2018.

[44] H. Hirai, "Settlements and stresses of multi-layered grounds and improved grounds by equivalent elastic method," *International Journal of Numerical Analysis and Modeling*, vol. 32, pp. 523–557, 2008.

[45] N. Loganathan and H. G. Poulos, "Analytical prediction for tunneling-induced ground movements in clays," *Journal of Geotechnical and Geoenvironmental Engineering*, vol. 124, no. 9, pp. 846–856, 1998.

[46] L. Q. Cao, D. L. Zhang, and Q. Fang, "Semi-analytical prediction for tunnelling-induced ground movements in multi-layered clayey soils," *Tunnelling and Underground Space Technology*, vol. 102, Article ID 103446, 2020.

[47] K. M. Lee, R. K. Rowe, and K. Y. Lo, "Subsidence owing to tunnelling. I. Estimating the gap parameter," *Canadian Geotechnical Journal*, vol. 29, pp. 929–940, 1992.

[48] Y. Q. Wu, K. Wang, L. Z. Zhang, and S Peng, "Sand-layer collapse treatment: an engineering example from Qingdao Metro subway tunnel," *Journal of Cleaner Production*, vol. 197, pp. 19–24, 2018.

[49] T. Hagiwara, R. J. Grant, M. Calvello, and R. N Taylor, "The effect of overlying strata on the distribution of ground movements induced by tunnelling in clay," *Soils and Foundations*, vol. 39, no. 3, pp. 63–73, 1999.

[50] R. B. Peck, "Deep excavations and tunneling in soft ground," in *Proceedings of the Seventh International Conference on Soil Mechanics and Foundation Engineering*, pp. 225–290, Mexico, MX, USA, August 1969.